8th International Symposium on Magnetic Bearing
August 26-28, 2002, Mito, Japan

A SIMPLE AND MINIATURIZED MAGNETIC BEARING FOR COST-SENSITIVE APPLICATIONS

Lichuan Li
Tadahiko Shinshi
Jiro Kuroki
Akira Shimokohbe
Precision and Intelligence Lab., Tokyo Institute of Technology, Yokohama, 226-8503 Japan
lcli@nano.pi.titech.ac.jp
shinshi@pi.titech.ac.jp
m0109kuroki@pms.titech.ac.jp
shimo@pi.titech.ac.jp

ABSTRACT
A standard magnetic bearing (MB) has active control of five motion axes, imposing significant complexity and high cost. In this paper we report a very simple and also miniaturized MB, including its design, fabrication and experiment test. In this MB the rotor is stabilized by active control of only its axial motion. The other four motion axes are passively stabilized using permanent magnets. In rotor radial translational motion, which is passively stabilized, a resonant frequency of 205 Hz is achieved for a rotor mass of 11.5×10^{-3} kg. This MB features virtually zero control current and zero rotor iron loss (hysteresis and eddy current losses). It is suitable for cost-sensitive applications such as cooling fans and auxiliary support for aerodynamic bearings.

INTRODUCTION
A standard MB with five axes actively controlled gives best performance but is expensive. In some applications the performance requirement is very moderate (such as a cooling fan), and a simplified MB is highly preferable for low cost. Simplicity (in particular, simple geometric structure) is also important for fabrication of small-size MBs, which is of increasing interest. There have been a lot of reports on the research and development of simple MBs. There have also been many techniques for simple MBs, including sensorless, tuned LC, and passive, as well as many modifications and extensions based on these basic ideas. The passive stabilization seems the simplest, which only involves specific geometric design of rotors and bearings and the use of permanent magnets (passive suspension by eddy current for a moving object is another case not included here).

Complete passive stabilization of a stationary object is impossible (Earnshaw's Law). However, it is possible for some of the motion axes to be passively stable. The remaining unstable motion axes then have to be actively controlled. There have been many papers reporting MBs involving the use of permanent magnets for passive stabilization of some of the axes. References [1]-[4] are only a few. The principle of our design is similar to that in [2][3]. Because only one axis is actively controlled, the simple MB is expected to be poor in performance. But it may still find application in places where even poor performance is enough. Cooling fan is an example. By using an MB a cooling fan can have much longer life-time and also lower noise, which is ideal for PCs and net servers.

DESIGN AND PARAMETERS
In passively stabilized axes, the stiffness is typically lower than that of actively controlled axes by a few orders, and to increase the stiffness is of great concern. The damping is also important but in passive axes it seems extremely difficult (if not impossible) to address this issue. One possibility for passive stabilization is to use the repulsive force between permanent magnets. In this case the magnets must interface with each other directly, without the presence of soft magnetic material. As a result, the flux density is limited by that of the permanent magnets, and the stiffness is only increased by using magnets of larger sizes. Repulsive force is also unfavorable due to the absence of closed flux loops; the magnets are being demagnetized by each other. Another possibility is to use tractive force, by which the motion in the directions that are parallel to the pole faces may be stable, as the case in a typical stepping motor. In this way soft magnetic material can be used to concentrate the flux for achieving a higher flux density (typically twice as much as that of merely permanent magnets), thus achieving a higher stiffness with similar sizes of the geometry. A high flux density is critical for high

stiffness since the stiffness is proportional to the square of flux density. In our design we use tractive force and permanent magnets plus soft magnetic material to give a concentrated flux.

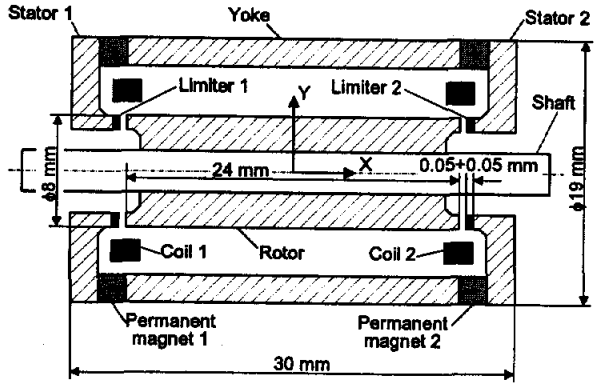

FIGURE 1: Design of a simple MB.

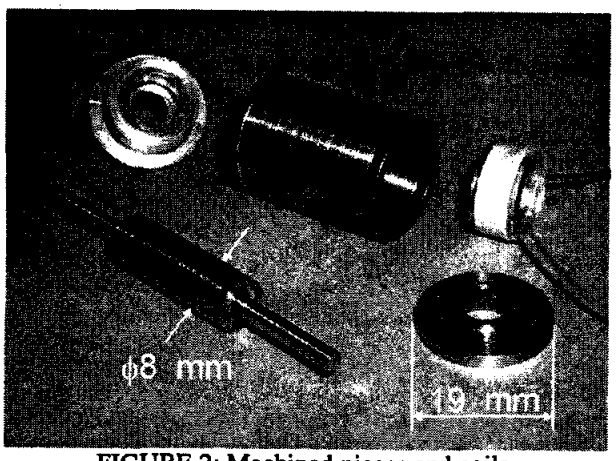

FIGURE 2: Machined pieces and coils.

The design is shown in Figure 1, where the rotor is found to be unstable only in the axial direction (the rotor has enough length-to-diameter ratio). The two coils are used to stabilize the rotor in the axial direction. The specific geometry is a result of extensive study based on experience, intuition, finite element analysis (FEA), and careful trade-offs. Fabrication of this MB is very easy. There are basically four mechanical parts to machine: a rotor, two identical stators, and a yoke, each being axial symmetric. They are machined on a general-purpose lathe. The required precision of machining is dependent on the rotational accuracy to be achieved. In our test case the errors of machining are tens of micrometers. According to the structure of the mechanical parts and the coils, it would not be difficult to use conventional machining techniques to make a much down-scaled one, e.g., a tenth of the present size. In the design, we have also considered the integration of a motor in the annular space between the two coils (not yet fabricated). The machined parts and the coils are shown in Figure 2. The shaft material is nonmagnetic stainless steel. The rotor, the stators and the yoke are made from solid soft iron (no lamination). The coil skeletons and the limiters (see Figure 1) are nonmagnetic and nonconductive. Material of the permanent magnets is NdFeB.

TABLE 1: Computed and measured parameters.

	Computed	Measured	
Position stiffness in X axis (Kx)	1.79×10^5	1.18×10^5	N/m
in Y axis (Ky)	2.45×10^4	1.91×10^4	N/m
about Z axis (Ky)	2.55	1.00	Nm/rad
Current stiffness in X axis (Ki)	3.74	3.02	N/A
Total coil turn (N)	$2\times100 = 200$	turns	
Total coil resistance (R)	$2\times1.8 = 3.6$	Ω	
Rotor Mass (m)	11.5×10^{-3}	kg	
Inertia moment, rotor+shaft, about Z axis (Jz)	1.96×10^{-6}	kgm^2	

We provide some more information about the design. Unless otherwise stated, all the data and descriptions are based on the equilibrium state: the state that the rotor is at the equilibrium position and is stationary, and the coil current is zero. According to the results from FEA, the flux density at the air gaps is a little greater than two Tesla. Thus the rotor and stator material near the air gaps is highly saturated, giving a stiffness in passive axes that is difficult to be further increased. There are four stiffnesses associated with the four passive axes: two translational and two rotational. Since the MB is rotationally symmetric, we consider the dynamics in the X-Y plane as shown in Figure 1. In this plane there are three stiffnesses: translational in the X axis (K_x) and Y axis (K_y), and rotational about Z axis (K_γ). The Z axis is perpendicular to the X-Y plane and points outward (not shown in Figure 1). Associated with the coils, which are connected in series, there is a current stiffness (K_i) for the X axis. Numerical values of these parameters from FEA are given in Table 1. Note that even if no explicit flux path is designed for coil fluxes, and the magnetic material near the air gaps is highly saturated, there is still a current stiffness that is enough for startup and control. Because K_x has a very large absolute value (see Table 1), it is important to check whether reasonable values of current can move the rotor from a limiting position (the rotor just touches one of the limiters) to the equilibrium position, which takes place at startup. Because at normal suspension the MB requires almost no power, a large power required only for startup would be unfavorable. With the data in Table 1, the current value for the rotor to start to go off a limiting position is $K_x X_l / K_i$ = 2.4 A, where X_l = 50 μm is the distance between the rotor at equilibrium position and a limiter (see Figure 1). At this current value, the DC power in the coils is 20.7 W. This power is high but only takes place at startup and persists for a couple of milliseconds.

Thus a charged capacitor can be used to provide the startup energy. In experiment test, similar startup current values are observed.

EXPERIMENT TEST

In this section we give some tested results on the simple MB we have introduced. The presented data contain enough information for judging the usefulness and also give us experience in such simple MBs.

Arrangement for Test

The open-loop dynamics of the rotor in the axial motion is a typical MB case: a magnetic force is approximated by a linear function of displacement and control current. The effect of eddy current in the bulky rotor and stator material is not considered. The parameters K_x and K_i are identified by finding out the minimum force (in axial direction) and the minimum current that push the rotor off a limiting position, by which the values of K_x and K_i can be calculated. They turn out to be smaller than what are given by FEA (see Table 1). A displacement sensor is used to detect rotor displacement in its axial direction, as shown in Figure 3. A first-order leading controller is used to stabilize the rotor. The rotor is suspended with a 600-Hz closed-loop bandwidth, giving a closed-loop stiffness in the axial direction that is well enough for applications such as a cooling fan. Rotor equilibrium position can be tuned to remove any dc component that may be present in the control current. The stabilizing control is not detailed. Our interest is primarily in the characteristics of those passive axes.

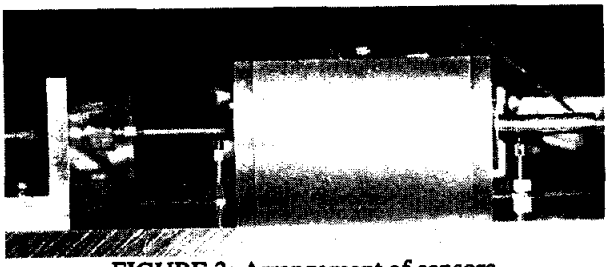

FIGURE 3: Arrangement of sensors.

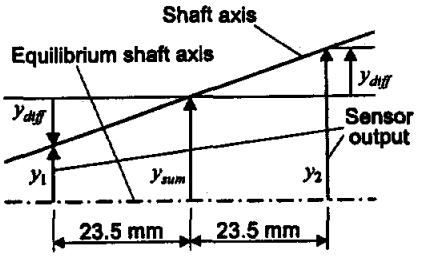

$$y_{sum} = \frac{y_1 + y_2}{2}, \quad y_{diff} = \frac{y_2 - y_1}{2}$$

FIGURE 4: Definition of variables.

The other two sensors in Figure 3 are used only for measurement. All the three sensors are of the same type (PU-150A, eddy-current gap sensor, 20 kHz bandwidth, 0.3 mm measuring range, manufactured by Advanced Electronic Corporation, Japan). The sensing coil has a diameter of 1.5 mm. The two sensors below the shaft measure the vertical displacement of the shaft at that point. With this arrangement, the sensors are verified to give satisfactory information of shaft displacement in vertical direction: a horizontal motion of 0.1 mm about the middle point gives rise to a sensor output of less than 1 μm (the shaft diameter is 3 mm). Sensor output are transformed as shown in Figure 4 into a sum y_{sum} and a difference y_{diff}, representing translational motion in the Y axis and rotational motion about the Z axis, respectively. Here we choose y_{diff} rather than an angular displacement since the latter may be very small and not readily judged.

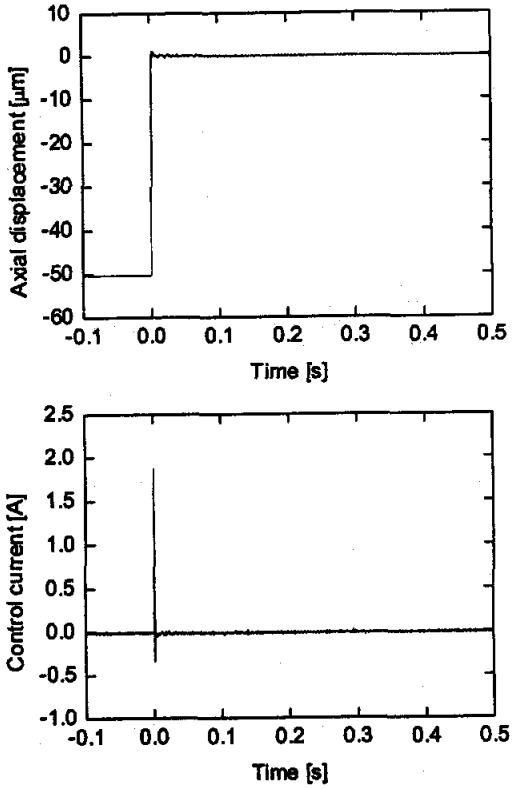

FIGURE 5: Startup transient.

Test of Startup

We are interested in the peak current in startup. Figure 5 gives the transient displacement and current at startup. The peak current is 1.88 A, and the transient dies out in about 1 ms. If we assume that the peak current persists identically for 1 ms through the coil resistance of 3.6 Ω, then the energy dissipated is found to be 0.013 J. This energy amounts to a discharge of a 1000-μF capacitor

from 15 V to 14 V. The magnetic energy is negligible, as the total coil inductance is 0.001 H (by measurement) and the associated magnetic energy is 0.002 J. We note that the control and measurement are carried out using a dSPACE DS1103 board and the associated software.

Test of Passive Axes

With the rotor suspended, an impact force is applied to the base of the MB. The response is shown in Figure 6. It is seen that the damping in the passive axes is very low, which is known to be a common phenomenon of passive suspension. The frequencies of the two vibration modes are found to be f_{sum} = 205 Hz in translational and f_{diff} = 114 Hz in rotational. Since the damping is low, these frequencies must be close to the natural resonant frequencies, by which the stiffnesses in the passive axes can be calculated. With the rotor mass in Table 1, the stiffness against translational motion is $K_y = m(2\pi f_{sum})^2 = 1.91\times10^4$ N/m, and that against rotational motion is $K_\gamma = J_z(2\pi f_{diff})^2 = 1.00$ Nm/rad. Compared with the FEA data (see Table 1), the difference in K_y may not be a surprise, while the difference in K_γ seems too big, of which the reason is unclear.

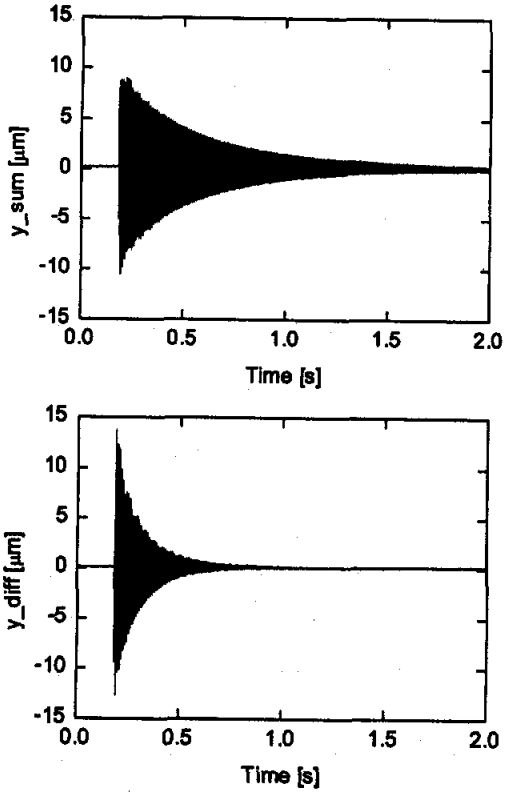

FIGURE 6: Impact response.

If we view the rotor as being supported by two linear springs, each with a stiffness of $K_y/2$ and locating along the X axis with a distance d, then according to the identified values of K_y and K_γ the distance is found to be $d = (4K_\gamma/K_y)^{1/2} = 14.5\times10^{-3}$ m. Note that d is obviously smaller than the 24-mm distance between the two air gaps at the ends of the rotor, where the stiffness against translational as well as rotational motion is generated. The value of d decreases with a decreasing rotor length and becomes zero at some finite rotor length.

Test of Rotation

At a rotational speed of 250 rpm, the signals y_{sum} and y_{diff} are shown in Figure 7. This fluctuation is found to be due to assembly errors between rotor and shaft (see evidence below). Inspecting these smooth sinusoidal signals, it is believed that the rotational precision is no worse than 1 μm. We note that no tachometer is used to measure rotor speed. It is obtained from the frequency of these fluctuating signals.

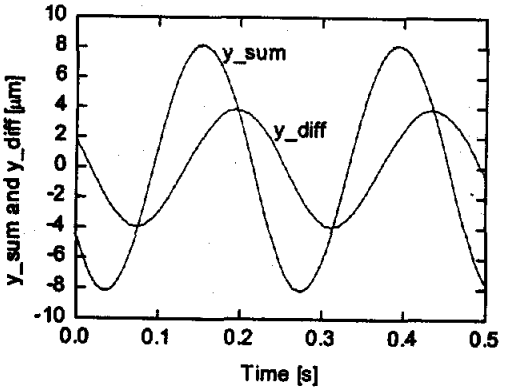

FIGURE 7: Vibration at low-speed rotation.

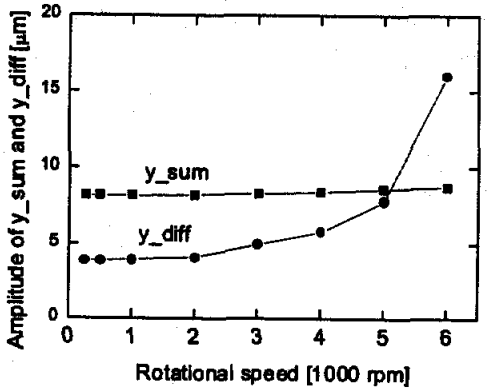

FIGURE 8: Vibration amplitude.

With a small blade glued on the shaft as an air turbine, the rotor is rotated at higher speeds. Figure 8 gives the amplitudes of y_{sum} and y_{diff} while rotating at several speeds. Note that for rotational speed from 250 up to 2000 rpm both the amplitudes are almost constant, indicating that the vibration in Figure 7 is caused by rotor-shaft assembly errors. At 6000 rpm, the amplitude of y_{diff} increases very rapidly with increasing rotor

speed. This is caused by the undamped 114-Hz (6840 rpm) mode. When we try to further increase the speed to cross this critical value, the rotor suddenly bursts into violent vibration and touches the stator, and the speed cannot be increased.

Finally, we give a test of rotor deceleration to judge the rotor loss. At a speed of 6000 rpm, the air supply is stopped. Then the rotor slows down as shown in Figure 9. The rate of slowing down is similar to that of a typical "full-size" MB, such as the slowing-down curve in [5], where the rotor has a mass of 3.3 kg and diameter of 80 mm. As the moment of inertia of a rotor is proportional to L^5 where L is a generalized rotor size, and the eddy current loss (which is usually the highest rotor iron loss) is proportional to the effective volume of rotor which is L^3 [6], and our small MB is about one tenth of typical sizes, the rotor loss is roughly as small as one hundredth of standard multi-pole-magnet MBs.

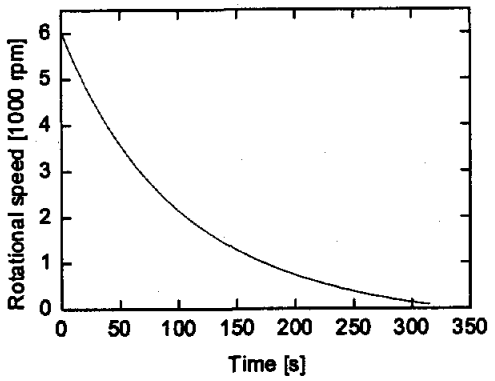

FIGURE 9: Rotor deceleration.

CONCLUSIONS

We have presented the design, fabrication and test of an MB with only one motion axis actively controlled. The MB is extremely simple in structure and can be easily manufactured at low cost. It provides a choice against conventional bearings in cost-sensitive applications.

The low damping in the passively stabilized motion axes is the main problem of such MBs. However, for small-size rotors a resonant frequency of more than 100 Hz is not difficult to achieve, thus rotational speed up to thousands of rpm is possible and application is not so limited.

Further studies include the integration of a motor and possible techniques for increase the damping and for the rotational speed to cross the critical values.

REFERENCES

1. S. Ueno, C. Chen, K.-I. Matsuda, Y. Okada and T. Masuzawa, Design of a Self-Bearing Slice Motor for a Centrifugal Blood Pump, Proc. of the 6th Int. Symp. on Magnetic Bearings, MIT, USA, Aug. 5-7, 1998, pp. 143-151
2. M. Komori, H. Kobayashi, and M. Kumamoto, Dynamic Characteristics of a Millimeter-Sized Magnetic Bearing with a Cylindrical Rotor, Proc. of the 6th Int. Symp. on Magnetic Bearings, MIT, USA, Aug. 5-7, 1998, pp. 152-161
3. M. Komori and T. Yamane, Micro PM Motors Levitated by Two Types of Active Magnetic Bearings, Proc. of the 7th Int. Symp. on Magnetic Bearings, ETH Zurich, Switzerland, Aug. 23-25, 2000, pp. 95-100
4. D.-C. Pang, J.-L. Lin, S.-C. Chen, B.-Y. Shew, and R. B. Zmood, Design, Fabrication, and Testing of a Millimeter-Level Magnetically Suspended Micromotor, Proc. of the 7th Int. Symp. on Magnetic Bearings, ETH Zurich, Switzerland, Aug. 23-25, 2000, pp. 105-110
5. X. Zhang, T. Shinshi, L. Li, K.-B. Choi, and A. Shimokohbe, Precision Control of Radial Magnetic Bearing, Proc. of the 10th Int. Conf. on Precision Engineering, Yokohama, Japan, July 18-20, 2001, pp. 714-718
6. P. E. Allaire, M. E. F. Kasarda, and L. K. Fujita, Rotor Power Losses in Planar Radial Magnetic Bearings - Effects of Number of Stator Poles, Air Gap Thickness, and Magnetic Flux Density, Proc. of the 6th Int. Symp. on Magnetic Bearings, MIT, USA, Aug. 5-7, 1998, pp. 383-391